Capacitive Bioanodes Enable Renewable Energy Storage in Microbial Fuel Cells

ARTICLE *in* ENVIRONMENTAL SCIENCE & TECHNOLOGY · MARCH 2012

Impact Factor: 5.33 · DOI: 10.1021/es204126r · Source: PubMed

4 AUTHORS, INCLUDING:

Tom H J A Sleutels
Wetsus
25 PUBLICATIONS **925** CITATIONS
SEE PROFILE

H.V.M. Hamelers
Wetsus
182 PUBLICATIONS **8,570** CITATIONS
SEE PROFILE

Cees Buisman
Wageningen University
236 PUBLICATIONS **6,268** CITATIONS
SEE PROFILE

Environmental Science & Technology

Article

pubs.acs.org/est

Capacitive Bioanodes Enable Renewable Energy Storage in Microbial Fuel Cells

Alexandra Deeke,*[,†,‡] Tom H. J. A. Sleutels,[‡] Hubertus V. M. Hamelers,[‡] and Cees J. N. Buisman[†,‡]

[†]Sub-Department of Environmental Technology, Wageningen University, Bornse Weilanden 9, P.O. Box 17, 6708 WG Wageningen, The Netherlands

[‡]Wetsus, Centre of Excellence for Sustainable Water Technology, Agora 1, P.O. Box 1113, 8900 CC Leeuwarden, The Netherlands

Supporting Information

ABSTRACT: We developed an integrated system for storage of renewable electricity in a microbial fuel cell (MFC). The system contained a capacitive electrode that was inserted into the anodic compartment of an MFC to form a capacitive bioanode. This capacitive bioanode was compared with a noncapacitive bioanode on the basis of performance and storage capacity. The performance and storage capacity were investigated during polarization curves and charge−discharge experiments. During polarization curves the capacitive electrode reached a maximum current density of 1.02 ± 0.04 A/m^2, whereas the noncapacitive electrode reached a current density output of only 0.79 ± 0.03 A/m^2. During the charge−discharge experiment with 5 min of charging and 20 min of discharging, the capacitive electrode was able to store a total of 22 831 C/m^2, whereas the noncapacitive electrode was only able to store 12 195 C/m^2. Regarding the charge recovery of each electrode, the capacitive electrode was able to recover 52.9% more charge during each charge−discharge experiment compared with the noncapacitive electrode. The capacitive electrode outperformed the noncapacitive electrode throughout each charge−discharge experiment. With a capacitive electrode it is possible to use the MFC simultaneously for production and storage of renewable electricity.

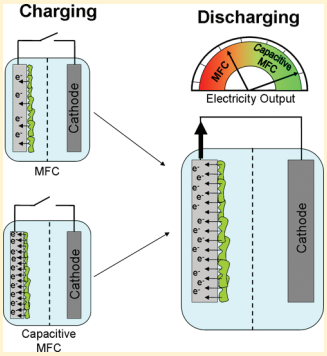

INTRODUCTION

Energy production from renewable energy sources receives more and more attention, because of the depletion of fossil fuels and the social urgency to decrease greenhouse gas emissions. Sun, wind, and biomass are huge renewable energy sources, available all over the world.[1,2] However, when using sun and wind as sources, it becomes difficult to match supply and demand of energy because of fluctuation of both demand and availability of renewable resources (e.g., day/night cycle, variable wind speeds). This is especially true for energy in the form of electricity, as an electrical grid has low intrinsic storage capabilities. Electricity storage capacity is a good option to match electricity production with the demand of the electricity market.[3] The advantage of biomass as a source for renewable energy is its worldwide availability and storage possibility. Storage, however, is only practical for biomass with high organic concentrations (low water volumes) because of the required storage capacity. An example for biomass with low organic concentrations (high water volumes) is wastewater. Wastewater is produced continuously all over the world, and even though it contains low organic concentrations it is an attractive source for sustainable electricity production from a microbial fuel cell (MFC).

The MFC is a recently developed technology for production of renewable energy, which can efficiently convert organic matter from wastewater into electricity.[4] The mechanism of an MFC is described in ref 5. To harvest more energy from the MFC, either the MFC would have to be disconnected at certain times or storage of the produced electricity would be required. Production of electricity in an MFC would be more attractive with a possibility to store electricity. Hence, we investigated the use of a capacitive bioanode in an MFC as a storage option for renewable energy from wastewater.

Electrochemical capacitors (ECs) are the most widely used capacitors to store electricity. ECs consist of two electrodes that are separated by a spacer material and an electrolyte. In an EC, electricity is stored as charge at the electrical double layer interphase between the electrode and electrolyte.[6]

Dewan et al.[7] performed a study on the use of an MFC with and without an external capacitor. The MFC was continuously operated when working without an external capacitor, and it was operated in batch mode with an external capacitor. This study showed that more energy could be harvested when the MFC was operated with an external capacitor. Another study on the use of external capacitors with an MFC has been performed by Kim et al.[8] They used four MFCs and eight capacitors to build a stack. The capacitors were charged in parallel and discharged in series. They also observed an increase in the peak power production of the MFCs when used with a capacitor. Use of an internal capacitor in an MFC however has not been tested before.

Received: November 18, 2011
Revised: February 11, 2012
Accepted: February 14, 2012

   dx.doi.org/10.1021/es204126r | Environ. Sci. Technol. XXXX, XXX, XXX−XXX

The goal of this research is the integration of a capacitive electrode with the bioanode. Such an integrated system would not require the use of an external capacitor. Microorganisms are expected to grow on the capacitive electrode and thereby to transfer the produced electrons into the capacitive electrode.

In terms of costs and material use, the integrated system has advantages compared to a system with an external capacitor, because there is no need for an additional spacer or electrolyte. The membrane, which is already present in the MFC to separate the anodic and cathodic compartments, is used as a separator (spacer) for the capacitor. The wastewater, which is used to feed the microorganisms in the anodic compartment, is used as an electrolyte. Furthermore, this integrated system requires only one electrode for the capacitor.

The feasibility to grow microorganisms on the capacitive electrode was studied, and the performance and energy storage were compared with the performance and energy storage of a noncapacitive bioanode.

MATERIALS AND METHODS

Electrochemical Cell Setup. Four identical cells, which were similar to cells used in recent published work,[9] were used in our experiments. The two compartments were separated by a cation exchange membrane. The electrode of each compartment was situated opposite the membrane. A plain graphite plate electrode (Müller & Rössner GmbH, Troisdorf, Germany) was used as the cathode. As the anode, two different types of electrodes were used, a noncapacitive (plain graphite plate) electrode and a capacitive electrode, consisting of a current collector (plain graphite plate electrode) coated with a capacitive layer. The anode, cathode, and membrane had a projected surface area of 22 cm^2.

Electrode Preparation and Analysis. The capacitive layer that was coated on the current collector consisted of a mixture of activated carbon powder and a polymer solution. The polymer solution was a mixture of NMP (*N*-methyl-2-pyrrolidone; Boom, Meppel, The Netherlands) and PVDF (poly(vinylidene fluoride); Kynar, Arkema, Amersfoort, The Netherlands). After the two components were mixed, the mixture was kept in an oven at 50 °C for at least 4 days, where it formed a homogeneous solution and was deaerated. The polymer solution was placed in a ball mill grinder (PM 100, Retsch, Haan, Germany) together with activated carbon powder (DLC Super 30, Norit, Amersfoort, The Netherlands) and extra NMP as a solvent. Mixing was done at 450 rpm for 30 min to ensure homogeneity of the mixture. After grinding, the capacitive paint was kept in an oven at 50 °C for 24 h for deaeration.

Before the capacitive layer was coated on the electrode, the current collector was roughened with sandpaper, rinsed with distilled water, and blow-dried with pressurized air. Capacitive paint was coated on the current collector at a thickness of 500 μm using a casting knife (stainless steel, 500 μm). Finally, the coated current collector was placed in an oven at 50 °C for 48 h for drying.

A small fraction of the capacitive paint was coated on a glass plate at the same thickness of 500 μm to investigate specific surface area. Gas adsorption analysis was carried out to determine the specific surface area (m^2/g) using the Brunauer–Emmett–Teller (BET) adsorption model according to ref 10.

An atomic force microscope (NanoScope Illa, Veeco, Santa Barbara, CA) was used to determine the roughness of each electrode surface. The atomic force microscopy (AFM) scan was performed on 2.5 mm^2 of each electrode surface. The pore size distribution on the surface of each electrode was analyzed with a scanning electron microscope (JEOL Technics Ltd., Tokyo, Japan). AFM pictures and scanning electron microscopy (SEM) pictures were captured for three different positions on each electrode surface to get a representative overview.

Operation and Measurements. The catholyte of the MFCs consisted of 100 mM ferricyanide solution. The anolyte consisted of 10 mM sodium acetate solution and 10 mM phosphate buffer solution. Additional supplies fed to the anolyte were 10 mL/L macronutrient solution containing 4.31 g/L NH_4Cl, 5.37 g/L $MgSO_4 \cdot 7H_2O$, and 4.31 g/L $CaCl_2 \cdot 2H_2O$, 1 mL/L micronutrient solution, and 1 mL/L vitamin solution as described in ref 11. Anolyte was continuously supplied at an inflow rate of 1.3 mL/min. Both anolyte and catholyte were circulated over the respective compartments at a flow rate of 100 mL/min. Anolyte was inoculated with effluent from another active MFC run on acetate.[12] The temperature of all cells was controlled at 30 °C using a water bath (K10, Thermo scientific, Geel, Belgium). The cells were operated at controlled anode potential with a potentiostat (N-stat, Ivium Technologies, Eindhoven, The Netherlands). The anode potential was set to −0.400 V (vs Ag/AgCl + 0.2 V vs NHE), Pro Sense, Oosterhout, The Netherlands) as the optimal working potential (determined during earlier experiments) for the microorganisms on the anode.[13] The pH in the anode compartment was constantly measured by a pH electrode (Liquisys, Endress + Hauser, Naarden, The Netherlands). During MFC operation, the voltage and current were constantly measured and the anode potential was controlled unless stated otherwise. The cells were run for 150 days at a controlled potential of −0.400 V. During the 150 days of operation, performance was analyzed on each cell by polarization curves and charge–discharge experiments. The polarization curves were measured at day 75, day 106, and day 145 of the MFC operation, and between the polarization curves, the charge–discharge experiments were measured.

All electrochemical measurements were conducted with the same potentiostat as indicated before. Polarization curves were performed to determine current output as a function of the anode potential. During the polarization curve the anode potential was varied in the range from −0.450 to −0.250 V in steps of 0.050 V. The anode potential was kept at each value for 10 min to reach a stable current output. The stable current density for each anode potential was taken from the average of stable current output from the last minute at each potential.

During charge–discharge experiments, control of the anode potential was alternated with an open circuit condition. The open circuit condition was used as the charging period for the cells. During the discharging period the cells were operated at a set anode potential of −0.300 V. This potential was chosen according to the highest current density from the noncapacitive electrode from polarization curves. For charge–discharge experiments, different sets of charge and discharge periods have been performed, which were consecutively repeated 15 times. As a first charge–discharge experiment, 10 min (charging) and 20 min (discharging) were chosen and compared with 20 min (charging) and 10 min (discharging) to investigate whether the charging or discharging period needs to be longer. Afterward, the charging period and the discharging period were varied. It was investigated whether longer charging and discharging periods would influence the stable operation of the electrodes during the cycling experiments (open circuit and control of the anode potential). For this purpose charging periods of 30 and 60 min and discharging periods of 60, 90, and 120 min were chosen. All periods which were used for charging and discharging of the cells are given in Table 1.

dx.doi.org/10.1021/es204126r | *Environ. Sci. Technol.* XXXX, XXX, XXX–XXX

Table 1. Schedule for the Charge−Discharge Experiments[a]

Discharging Period (min) \ Charging Period (min)	5	10	20	30	60
10	x	nd	x	nd	nd
20	x	x	nd	nd	nd
60	nd	nd	nd	x	nd
90	nd	nd	nd	nd	x
120	nd	nd	nd	nd	x

x Determined

nd Not determined

[a]The yellow shading indicates where experiments have been performed.

Calculations. During the experiments, three situations can be distinguished: steady-state current output, charging, and discharging. The origin of the current during each situation is further described in Figure 1a. The measured current (i_m, A) is the current that flows from the anode to the cathode and therefore can be measured for both the noncapacitive and the capacitive electrodes. The produced current (i_p, A) is defined as the current produced by the microorganisms and stored on the electrode during the charging period.

Steady-state current output is reached during the last minute at each potential of the polarization curves, where the produced current is equal to the measured current ($i_p = i_m$).

During the charging period, when the electric circuit is open, the measured current is zero and the produced current is stored as charge on the capacitive electrode:

$$i_m = 0 \qquad i_p = \frac{dQ_s}{dt} \tag{1}$$

where Q_s is the stored charge (C).

During the discharge period, the measured current is equal to the produced current plus the stored charge (see Figure 1b):

$$i_m = i_p + \frac{dQ_s}{dt} \tag{2}$$

Because it is impossible to distinguish between the amount of produced current and stored charge, further calculations are made to determine the amount of measured charge. The measured charge (Q_m, C) is the integral of the current curve from the charge−discharge experiment (shaded area in Figure 1b):

$$Q_m = \int_0^{t_o} i_m dt \tag{3a}$$

Substituting the measured current in eq 3a leads to

$$Q_m = \int_{t_c}^{t_o} \left(i_p + \frac{dQ_s}{dt} \right) dt \tag{3b}$$

$$Q_m = i_p(t_o - t_c) + \Delta Q_s \tag{3c}$$

where t_o is the overall time of the charge−discharge cycle (s) and t_c is the charging time (s). The expected charge is calculated as

$$Q_{cont,d} = i_s t_d \tag{4}$$

where $Q_{cont,d}$ is the expected charge (C), i_s is the steady-state current (A) from the noncapacitive electrode taken from the polarization curves at an anode potential of −0.300 V, and t_d is the discharge time ($t_d = t_o - t_c$) (s).

To assess the effectiveness of each electrode, the charge recovery (η_{rec}) is introduced:

$$\eta_{rec} = \frac{\sum Q_{m,k}}{nQ_{cont,d,k}} \tag{5}$$

The charge recovery relates the measured charge from each experiment to the expected charge for each experiment. $Q_{cont,d}$ is the expected charge (C), n is the number of cycles, and $\sum Q_{m,k}$ is the sum of the measured charge of each cycle (cumulative total charge) (C).

Charge recovery can reach three different states: (a) $\eta_{rec} \leq 1$, (b) $\eta_{rec} = 1$, and (c) $\eta_{rec} \geq 1$. When charge recovery is smaller than 1, the measured charge is lower than the expected charge.

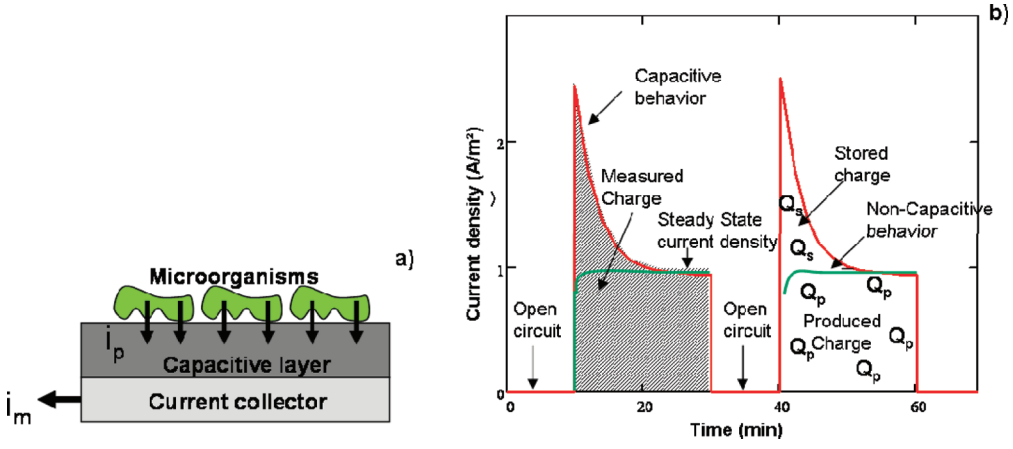

Figure 1. (a) Current distribution between microorganisms and the electrode, showing the origin of the measured and the produced currents. (b) Theoretical discharge graph, giving the measured charge as the shaded area underneath the current density graph. The measured charge can be split into the stored charge (area of the peak above the noncapacitive behavior line) and the produced charge (area underneath the noncapacitive behavior line).

dx.doi.org/10.1021/es204126r | Environ. Sci. Technol. XXXX, XXX, XXX−XXX

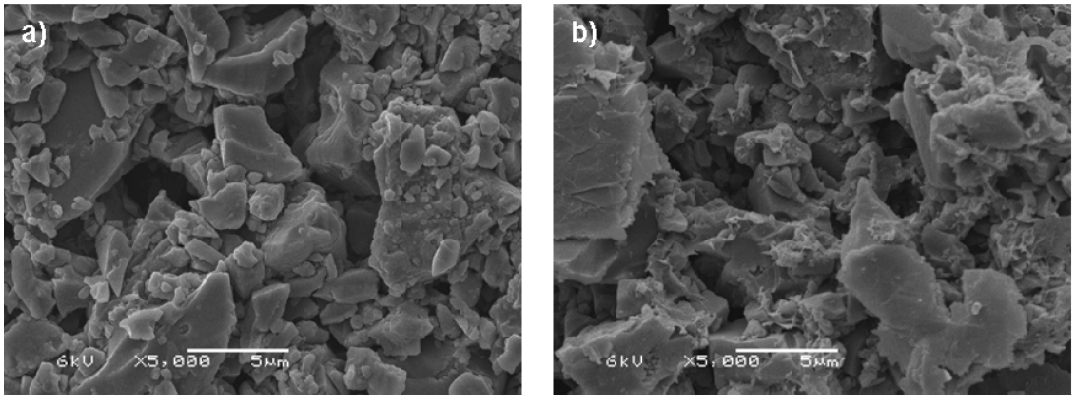

Figure 2. (a) SEM picture showing the top view of the capacitive electrode. (b) SEM picture showing the cross-sectional view of the capacitive electrode.

When charge recovery is equal to 1, the measured charge is equal to the expected charge, and when charge recovery is bigger than 1, the measured charge is bigger than the expected charge.

RESULTS AND DISCUSSION

The difference in performance of the capacitive and noncapacitive electrodes was determined using different techniques. First, the pore size distribution was determined using SEM and AFM. Then electrochemical properties were determined by recording potential scans, and finally, the charge−discharge behavior of both electrodes was investigated.

Characterization of the Capacitive Electrode. The pore size distribution was analyzed using AFM and SEM. SEM pictures of the capacitive electrode are given in Figure 2. The top view of the capacitive electrode is given in Figure 2a, and the cross-sectional view of the capacitive electrode is given in Figure 2b. Both figures show that carbon particles and polymer binder are well mixed. The SEM pictures showed a pore size distribution of 5 μm on the electrode surface. The cross-sectional view showed that the depth of the pores of the capacitive electrode ranged from 5 to 10 μm. The noncapacitive electrode had a pore size distribution of 2 μm on the electrode surface. AFM images confirm the typical pore size distribution found in the SEM images. Pictures obtained from the AFM analysis are given in the Supporting Information. The capacitive electrode was coated with 500 μm; due to evaporation of the solvent during the drying process, the electrode shrank down to a thickness of 220 μm. BET analysis of the capacitive electrode revealed a specific surface area of 1081 m^2/g. Both SEM pictures and AFM pictures show that the capacitive electrode has a rougher electrode surface than the noncapacitive electrode.

Electrochemical Characterization of the Biofilm. Electrochemical characterization of the biofilm was done by polarization curves. The obtained polarization curves are given in Figure 3. The noncapacitive electrode reached a maximum current density of 0.79 ± 0.03 A/m^2 at an anode potential of −0.300 V. Even though the anode potential was further increased to −0.250 V, the current density decreased to 0.77 ± 0.03 A/m^2. The capacitive electrode had a current density increase throughout the whole anode potential range. The capacitive electrode reached a maximum current density of 1.02 ± 0.04 A/m^2 at an anode potential of −0.250 V. A negative current was observed for the capacitive electrode at an anode potential of −0.450 V even after this potential was maintained for 20 min. The capacitive electrode performed

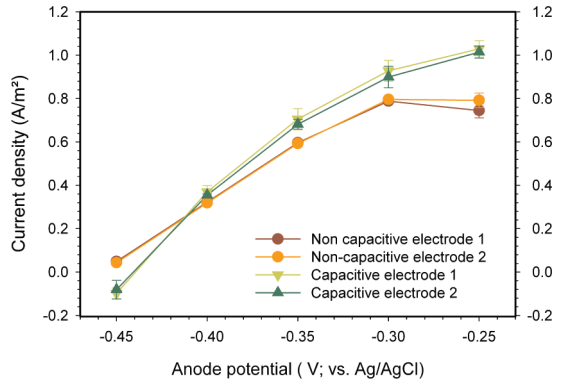

Figure 3. Polarization curves obtained from the different electrodes in an anode potential range of −0.450 to −0.250 V. There are clear differences in performance between the noncapacitive electrode and the capacitive electrode. The capacitive electrode reached a higher current density output of up to 1.02 A/m^2 compared with the current density output of 0.79 A/m^2 of the noncapacitive electrode.

better than the noncapacitive electrode in most of the applied anode potentials. This difference in performance could be due to the difference in roughness of the electrodes, because the surface of the capacitive electrode has an increased roughness compared with that of the noncapacitive electrode (see the section "Characterization of the Capacitive Electrode").

Charge−Discharge Experiments. During charge−discharge experiments the cells were controlled at open circuit, alternated with control of the anode potential at −0.300 V. The electrodes are charged when the electric circuit is open, and they are discharged when the anode potential is controlled. This charging−discharging was done at 12 different intervals to investigate possible time effects (Table 1). The potential behavior and the current density behavior for the charging (10 min) and discharging (20 min) are given in Figure 4. This figure is representative for all charge−discharge experiments. Figures for the other charge−discharge experiments are available in the Supporting Information.

Potential Behavior. The typical potential behavior of the charge−discharge experiment is given in Figure 4 a. After the electric circuit was opened, the initial potential drop from the noncapacitive electrode was around 0.110 V, whereas the initial potential drop from the capacitive electrode was 0.070 V. The potential from the noncapacitive electrode decreased to the final value of −0.480 V, the open circuit potential. The potential from the capacitive electrode dropped to a potential value

dx.doi.org/10.1021/es204126r | Environ. Sci. Technol. XXXX, XXX, XXX−XXX

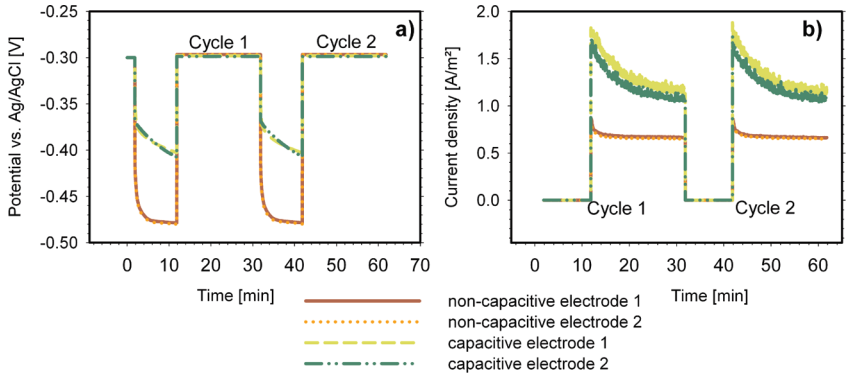

Figure 4. Typical potential (a) and current density (b) behavior for two cycles of a charge−discharge experiment with 10 min of charging and 20 min of discharging.

of around −0.410 V until the charging period ended. The potential from the capacitive electrode dropped slower than the potential from the noncapacitive electrode. The noncapacitive electrode showed an immediate potential drop to potentials lower than −0.450 V. Because this potential is comparable to the open circuit potential, this potential implies that the produced current is zero. Looking at the polarization curves confirms that the produced current at these potentials is zero. In the case of the capacitive electrode, the overall potential drop was smaller than that of the noncapacitive electrode; therefore, the produced current i_p was bigger then zero. This difference in potential behavior is due to the fact that electrons produced by the microorganisms are stored in the capacitive electrode. The capacitive electrode has a rougher surface than the noncapacitive electrode. Through this rougher surface the double layer capacitance of the capacitive electrode is increased compared with the double layer capacitance of the noncapacitive electrode. The capacitive electrode therefore reaches a different final potential compared with the noncapacitive electrode. The smaller potential drop behavior of the capacitive electrode compared with the noncapacitive electrode demonstrated that the capacitive electrode is able to store charge.

Current Density Behavior. The typical current density behavior of the noncapacitive and capacitive electrodes is given in Figure 4 b. All electrodes had a peak in current density after the electric circuit was closed. After this peak, the current density of each electrode decreased toward a stable current density. The height of this peak is related to the amount of charge that was stored according to eqs 3a, 3b, and 3c. The presence of a peak in the current density indicates that more charge was produced during the charging period than during continuous operation.

The noncapacitive electrode had a peak of 0.9 A/m^2 throughout each time interval. The height of the peak in current density of the noncapacitive electrode was in accordance with the potential drop during the charging period. The noncapacitive electrode had a quick drop in potential, which showed that only a small amount of charge was stored. Afterward the current density converged toward a stable value of 0.7 A/m^2 during each interval. The capacitive electrode had a higher peak current density of 1.7 A/m^2 during each interval compared to the noncapacitive electrode. This indicates that the amount of stored charge was larger for the capacitive electrode compared with the noncapacitive electrode. The stable current density output of the capacitive electrode was 1.15 A/m^2.

The noncapacitive electrode reached a stable current density output which was comparable with the polarization curves in Figure 3. Only a small amount of charge was stored on the noncapacitive electrode. Uría et al.[14] showed that a small amount of charge can be stored in the biofilm, which might be happening in the case of the noncapacitive electrode.

The capacitive electrode performed better during the charge−discharge experiments (1.15 A/m^2) than was expected from the polarization curves (0.93 A/m^2). Part of this better performance can be linked to the rougher surface of the capacitive electrode, but another part of the performance increase might be explained by the fact that storage of charge occurred. During the charging period, electrons are stored inside the electrode and the produced protons accumulate in the biofilm. During the discharging period, the electrons are released from the anode to the cathode and the accumulated protons are transported from the biofilm to the bulk solution. Since the protons are most likely transported out of the biofilm through the protonation of the conjugate base of the buffer,[15] immediate release of all stored protons (at closure of the electric circuit) would lead to an increase in buffer capacity at the biofilm, and this would enable a high current density output.

The performances of each electrode were also compared according to the average current density reached during cycling between the open electric circuit and potential control. This average current density during the cycled experiment (open circuit + closed circuit) was compared with the current density of constant operation. The current density value for constant operation was taken from the polarization curves at an anode potential of −0.300 V. The noncapacitive electrode reached a current density of 0.79 A/m^2 during the polarization curves. During the charge−discharge experiment the average current density was 0.41 A/m^2; this was 0.38 A/m^2 lower than during constant operation. The capacitive electrode reached a current density of 0.93 A/m^2 during the polarization curves. During the charge−discharge experiments the average current density was 0.76 A/m^2; this was only 0.17 A/m^2 lower than during continuous operation. This shows that an internal capacitor inside an MFC improves the relative performance compared with an MFC without internal storage capacity at discontinuous operation, which is in accordance with the work by Dewan et al.[7]

The capacitive electrode was able to produce 0.2 (kW h)/g (of activated carbon powder), which is comparable to that of other electrochemical capacitors.[16] This performance might be improved by choosing a different PVDF solution or a different activated carbon powder. Also the thickness of the capacitive

dx.doi.org/10.1021/es204126r | Environ. Sci. Technol. XXXX, XXX, XXX−XXX

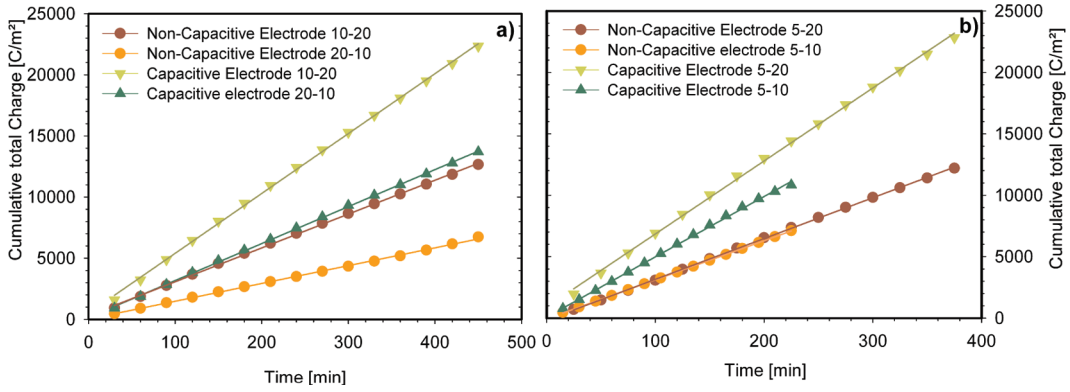

Figure 5. (a) The cumulative total charge from the charge−discharge experiments with a charging time of 10 min and discharging time of 20 min is compared with that from the charge−discharge experiments with a charging time of 20 min and a discharging time of 10. (b) The cumulative total charge from the charge−discharge experiments with 5 min of charging time and 20 min of discharging time is compared with that from the charge−discharge experiments with 5 min of charging time and 10 min of discharging time.

Table 2. Cumulative Total Charge (Q_m, C/m^2) of Each Experiment for the Noncapacitive and Capacitive Electrodes

	10 min−20 min	20 min−10 min	5 min−20 min	5 min−10 min	30 min−60 min	60 min−90 min	60 min−120 min
noncapacitive electrode	12665	6739	12195	7112	33743	59673	80895
capacitive electrode	22345	13688	22831	10819	56809	79750	128160

Table 3. Charge Recovery (η_{rec}) for the Noncapacitive Electrode and the Capacitive Electrode during Each Charge−Discharge Experiment

	10 min−20 min	20 min−10 min	5 min−20 min	5 min−10 min	30 min−60 min	60 min−90 min	60 min−120 min	av
noncapacitive electrode	0.870	0.874	0.894	0.368	0.791	0.933	0.948	0.811
capacitive electrode	1.571	1.925	1.606	1.522	1.332	1.246	1.502	1.529

electrode, which was casted with 500 μm, might have an influence on its performance.

Cumulative Total Charge. Cumulative total charge during each experimental interval was calculated according to eqs 3a, 3b, and 3c to gain further insights into the storage capacity, stability, and time effects of each electrode. The graph of cumulative total charge is given in Figure 5.

Under cycling conditions (open electric circuit and control of the anode potential) the stable operation of each electrode was tested. Therefore, each defined charge−discharge cycle has been repeated consecutively 15 times. The slope of each graph in Figure 5 represents the amount of measured charge for each single charge−discharge cycle. The amount of measured charge remained stable over each charge−discharge experiment for both electrodes; hence, the noncapacitive and the capacitive bioanodes are both able to cope with the cycling.

The effect of charging time and discharging time on the amount of cumulative total charge was investigated by performing experiments with different time settings. During the first set of charge−discharge experiments it was investigated whether the charging or the discharging of the electrode would take longer. The graphs of the cumulative total charge in Figure 5 reveal that the discharging of the electrode takes longer than the charging. The discharging process of the electrodes is slower than the charging process. Therefore, a long discharge time is required to enable the electrodes to release all the charge that was produced during the preceding charging period. Furthermore, these experiments showed that the capacitive electrode is able to produce more charge than the noncapacitive electrode.

After these shorter charge−discharge experiments, the charging and discharging times have been elongated in further experiments. The charging time was elongated to 60 min and the discharging time to 120 min. This elongation of the discharging times has been done to test whether the MFC can be used as a system for distributed energy generation. Schoenung et al.[17] defined a discharge time range of 0.5−4 h as a requirement for a suitable distributed energy generation system. A distributed energy generation system reaching this discharge time range can be used in the existing electrical grids for peaks in electricity requirement and load leveling. In Table 2 the comparison of the cumulative total charge for all experiments is given.

The cumulative total charge in Table 2 shows that the capacitive electrode was able to produce more charge than the noncapacitive electrode during each charge−discharge experiment. The graphs of the cumulative total charge for these experiments can be found in the Supporting Information.

The comparison of the ability to store charge of the noncapacitive electrode and the capacitive electrode was quantified through the charge recovery according to eq 5. The charge recovery is given in Table 3.

The charge recovery of the noncapacitive electrode was lower than 1 for most of the charge−discharge experiments. Thus, the measured charge of the noncapacitive electrode is lower than the expected charge. The charge recovery shows that on average the noncapacitive electrode produced 18.9% less charge than expected. During the charge−discharge experiment with 5 min of charging and 10 min of discharging, the noncapacitive electrode performed less than the average and achieved a charge recovery of only 37%. In this experiment, the open circuit condition is held for one-third of the whole charge−discharge cycle. The microorganisms delivered the electrons to the electrode with some delay after the electric circuit was closed; this caused the small charge recovery. In the charge−discharge

dx.doi.org/10.1021/es204126r | Environ. Sci. Technol. XXXX, XXX, XXX−XXX

experiments with 60 min (charging) and 90 and 120 min (discharging), the noncapacitive electrode reaches charge recoveries which are close to 1. This good performance could be due to the long working periods at the set anode potential. The electrodes are able to reach stable conditions.

The capacitive electrode performed better during all experiments and has higher values for the charge recovery compared with the noncapacitive electrode. For all experiments the charge recovery is higher than 1. On average the capacitive electrode produced 52.9% more charge than expected. From this 52.9% charge recovery around 18% can be assigned to improved performance of the capacitive electrode already measured during the polarization curves, where the noncapacitive electrode only achieved a current density of 0.79 A/m^2 and the capacitive electrode achieved 0.93 A/m^2. The remaining 35% of improved charge recovery is due to actual storage of charge taking place in the capacitive electrode as indicated in Figure 1b. This indicates that the integrated storage system with the capacitive electrode inserted into the anode compartment of an MFC is successful.

Perspectives. A system consisting of a capacitive electrode inside an MFC was compared to a system with a noncapacitive electrode. The capacitive system outperformed the noncapacitive system throughout each experiment. The capacitive electrode enabled the on-demand release of stored electrons. With the capacitive electrode we already have managed to receive 0.2 kWh/g (of activated carbon powder). This amount of electricity storage can be improved in the future by changing the composition and thickness of the capacitive electrode. Also charging and discharging periods need to be further improved to reach the required discharging time of 4 h for the distributed energy generation.

With a capacitive electrode it is possible to use the microbial fuel cell simultaneously for production and storage of renewable energy. This offers new possibilities for applications of the MFC.

■ ASSOCIATED CONTENT

Ⓢ Supporting Information

Figures showing and text describing the AFM images of the capacitive and nocapacitive electrodes, potential behavior and current density of the charge−discharge experiments, and cumulative total charge of the capacitive and nocapacitive electrodes. This material is available free of charge via the Internet at http://pubs.acs.org.

■ AUTHOR INFORMATION

Corresponding Author

*Phone: +31 58 2843190; fax: +31 58 2843001; e-mail: Alexandra.Deeke@wetsus.nl.

Notes

The authors declare no competing financial interest.

■ ACKNOWLEDGMENTS

This work was performed in the TTIW-cooperation framework of Wetsus, Centre of Excellence for Sustainable Water Technology (www.wetsus.nl). Wetsus is funded by the Dutch Ministry of Economic Affairs, the European Union European Regional Development Fund, the Province of Fryslân, the city of Leeuwarden, and the EZ-KOMPAS Program of the "Samenwerkingsverband Noord-Nederland". We thank the participants of the research theme "Bio-energy" for the fruitful discussions and their financial support. Special thanks go out to Annemiek ter Heijne and Philipp Kuntke for critical reading of this paper and to Michel Saakes for the support in the laboratory.

■ REFERENCES

(1) Moomaw, W. Renewable energy and climate change: an overview. *IPCC Scoping Meeting on Renewable Energy Sources—Proceedings*; Intergovernmental Panel on Climate Change: Geneva, Switzerland, 2008: pp 3−32.

(2) Berndes, G.; Hoogwijk, M.; van den Broek, R. The contribution of biomass in the future global energy supply: a review of 17 studies. *Biomass Bioenergy* **2003**, *25* (1), 1−28.

(3) Pickard, W. F.; Shen, A. Q.; Hansing, N. J. Parking the power: strategies and physical limitations for bulk energy storage in supply-demand matching on a grid whose input power is provided by intermittent sources. *Renewable Sustainable Energy Rev.* **2009**, *13* (8), 1934−1945.

(4) Aelterman, P.; Rabaey, K.; Clauwaert, P.; Verstraete, W. Microbial fuel cells for wastewater treatment. *Water Sci. Technol.* **2006**, *54* (8), 9−15.

(5) Logan, B. E.; Hamelers, B.; Rozendal, R.; Schröder, U.; Keller, J.; Fregula, S.; Aelterman, P.; Verstraete, W.; Rabaey, K. Microbial fuel cells: methodology and technology. *Environ. Sci. Technol.* **2006**, *40* (17), 5181−5192.

(6) Obreja, V. V. N. On the performance of supercapacitors with electrodes based on carbon nanotubes and carbon activated material—a review. *Physica E* **2008**, *40* (7), 2596−2605.

(7) Dewan, A.; Beyenal, H.; Lewandowski, Z. Intermittent energy harvesting improves the performance of microbial fuel cells. *Environ. Sci. Technol.* **2009**, *43* (12), 4600−46.

(8) Kim, Y.; Hatzell, M. C.; Hutchinson, A. J.; Logan, B. E. Capturing power at higher voltages from arrays of microbial fuel cells without voltage reversal. *Energy Environ. Sci.* **2011**, *4* (11), 4662−4667.

(9) ter Heijne, A.; Hamelers, H. V. M.; Saakes, M.; Buisman, C. J. N. Performance of non-porous graphite and titanium-based anodes in microbial fuel cells. *Electrochim. Acta* **2008**, *53* (18), 5697−5703.

(10) Atkins, P. W. *Physical Chemistry*; VCH-Wiley-Interscience: Weinheim, Germany, 1990; Vol. *1*.

(11) ter Heijne, A.; Hamelers, H. V. M.; Buisman, C. J. N. Microbial fuel cell operation with continuous biological ferrous iron oxidation of the catholyte. *Environ. Sci. Technol.* **2007**, *41* (11), 4130−4134.

(12) Sleutels, T. H. J. A.; Lodder, R.; Hamelers, H. V. M.; Buisman, C. J. N. Improved performance of porous bio-anodes in microbial electrolysis cells by enhancing mass and charge transport. *Int. J. Hydrogen Energy* **2009**, *34* (24), 9655−9661.

(13) Logan, B. E.; Regan, J. M. Microbial fuel cells: challenges and applications. *Environ. Sci. Technol.* **2006**, *40* (17), 5172−5180.

(14) Uría, N.; Berbel, X. M.; Sánchez, O.; Muñoz, F. X.; Mas, J. Transient storage of electrical charge in biofilms of *Shewanella oneidensis* MR-1 growing in a microbial fuel cell. *Environ. Sci. Technol.* **2011**, *45* (23), 10250−10256.

(15) Torres, C. I.; Kato Marcus, A.; Rittmann, B. E. Proton transport inside the biofilm limits electrical current generation by anode-respiring bacteria. *Biotechnol. Bioeng.* **2008**, *100* (5), 872−881.

(16) Hall, P. J.; Mirzaeian, M.; Fletcher, S. I.; Sillars, F. B.; Rennie, A. J. R.; Shitta-Bey, G. O.; Wilson, G.; Cruden, A.; Carter, R. Energy storage in electrochemical capacitors: designing functional materials to improve performance. *Energy Environ. Sci.* **2010**, *3* (9), 1238−1251.

(17) Schoenung, S. M. Hassenzahl, W.V. *Long vs. Short-Term Energy Storage: Sensitivity Analysis. A Study for the DOE Energy Storage Systems Program*; Sandia National Laboratories: Livermore, CA, 2007.